APPLIED AND ENVIRONMENTAL MICROBIOLOGY, Nov. 1996, p. 3985–3990 Vol. 62, No. 11
0099-2240/96/$04.00+0

Formation of 30- to 40-Micrometer-Thick Laminations by High-Speed Marine Bacteria in Microbial Mats

GREGORY M. BARBARA* AND JAMES G. MITCHELL

Biological Sciences, Flinders University, Adelaide, South Australia 5001, Australia

Received 22 May 1996/Accepted 6 September 1996

The precision with which motile heterotrophic bacteria could position themselves in microbial mats was determined. This required the development of a technique to view motile bacteria in situ. This was successfully achieved by replacing a 1-cm-diameter minicore from the mat sediment with 210- to 300-μm-diameter glass beads or sieved agar. After allowing 3 days for regrowth of the mat into the transparent medium, a cross section showed that bacteria formed a layer as thin as 30 to 40 μm at a depth of 500 μm below the surface. Bacterial concentrations in this microlamination were 20 times above background. Mean speeds were 200 μm s^{-1} inside and 60 μm s^{-1} outside the microlamination. The percentages of bacteria turning per 30 s were 93% inside and 10% outside the microlamination. Artificial chemical gradients were unsuccessful in stimulating microlamination formation or in eliciting the same extent of speed and turning responses. The significance of the results is that it is now possible to microscopically examine sedimentary bacteria in situ. Our first examination indicates that some bacteria form chemotactic microlaminations by increasing their turning frequency. This behavior is opposite that described in the enteric-based model of chemotactic movement, in which positive chemotaxis is achieved by decreasing the turning frequency.

The term microbial mats describes a variety of microbial communities that grow on aquatic sediments or solid surfaces to form distinct layered structures (2). Their matrix is formed by filamentous bacteria (6), and the resultant structure is usually laminated, not only on a scale visible to the naked eye but also at the micrometer level (3, 12). The laminations reflect a vertical stratification of both the physiological attributes of the microbial components and the associated physicochemical regimes (3). Typically, the surface layer is composed of cyanobacteria and photosynthetic eukaryotes underlain by thin layers of nonoxygenic phototrophic bacteria and heterotrophic bacteria (9). The oxygenic photosynthetic bacteria produce oxygen, which is rapidly reduced by organic-matter oxidizers and sulfide oxidizers. Below the oxidizers, in the anaerobic zone, the remaining organic matter is reduced by sulfate-reducing bacteria, which produce hydrogen sulfide (H_2S). The production of H_2S turns the mud beneath mats black, through the production of FeS. The photosynthesis in the mats is not all oxygenic. Purple sulfur bacteria in the anaerobic zone carry out anoxygenic photosynthesis, in which H_2S rather than water is used as an electron donor and sulfur replaces oxygen as the oxidized product (5). Hence, a mature microbial mat exhibits zones of aerobic and anaerobic photosynthesis.

Microbial mats are dynamic systems with dramatic fluctuations of oxygen and sulfide gradients during a diurnal cycle (10). Because of the very high biological activity within the mats, extremely steep gradients in the concentrations of oxygen and soluble sulfide are characteristic of the mats' depth profile (12, 17). This leads to productive mats in protected shallow-water regions often becoming anaerobic almost to the surface, with the anaerobic zone extending into the overlying water column at night (9). Because of these fluctuations in potentially harmful conditions (e.g., sulfide usually inhibits oxygenic photosynthesis strongly, and oxygen is often poisonous to anaerobic microorganisms), bacteria may develop avoidance or defense mechanisms to optimize fitness and competitive ability (12). One mechanism by which bacteria might optimize fitness in the presence of dynamic gradients is to avoid extremes or migrate to optimal conditions within the gradient, or both. Therefore, the laminations within a mat may reflect the growth and/or tactic responses of the constructing microorganisms.

Motility is a major tactic utilized by bacterial cells to enhance their survival directing the bacteria to nutrient sources and away from toxic or low-nutrient environments (4). In flagellated bacteria this is achieved in the form of a biased random walk (4). This response to chemical concentration gradients is known as chemotaxis (1). Superior motility and chemotaxis of cells in mixed cultures can enhance the competitive fitness of bacteria, even in the presence of faster-growing species (13). Therefore, the ability of heterotrophic bacteria within mats to respond quickly to dynamic fluctuations in nutrient and toxic-compound levels is extremely important for the survival and growth of the bacteria.

Previously, the focus of bacterial motility studies has been on specific species and isolates, while the motility of mixed communities has not been studied in such detail (16). Therefore, there is currently little information on community motility and chemotaxis within microbial mats. Motility studies on isolated bacteria associated with microbial mats (8, 11, 15) show that the motility of mat bacteria may be influenced by oxygen and sulfide concentrations. The phototrophic purple sulfur bacterium *Chromatium minus* responded immediately to the addition of sulfide. The cells either increased or decreased their velocity depending on whether sulfide was initially absent or present in the medium (15). In laboratory trials, the bacterium *Thiovulum majus* reorients itself within a preferred oxygen gradient (8, 11, 12) and may form specific bands within mat sediments (12).

In the past, because of the organosedimentary structure of the mats, it has been difficult to observe and quantify bacterial motility, which had led to migration rates being based on qualitative observations (12). This paper describes the development of a technique for the in situ determination of the

* Corresponding author. Mailing address: Biological Sciences, Flinders University, P.O. Box 2100, Adelaide, SA 5001, Australia. Phone: (61-8) 201-3812. Fax: (61-8) 201-3015. Electronic mail address: Jim.Mitchell@cc.flinders.edu.au.

swimming speed and distribution of the heterotrophic bacterial community within a mat to a spatial resolution of 10 μm. Additionally, the relationship between the gradient (O_2 and H_2S)-dominated system and bacterial migration was investigated by experimentally manipulating chemical concentrations within a mat and measuring the oxygen gradient within the microbial mat to define the limits of oxygen penetration.

MATERIALS AND METHODS

The St. Kilda mangrove trail in South Australia was selected as the study site for this project. The mangrove forest provides the mats with a high input of organic matter and protection from physical factors that could rework the sediment. Bioturbation by invertebrates is minimal because of the high sulfide concentrations. The development of oxygen and sulfide gradients within the mats is further aided by isolation from most tides, leading to hypersalination (40 to 60 ‰) and stagnation of the overlying water column.

Motility examination. Because the bacteria live in opaque sediment, it was necessary to replace some of the sediment with a translucent medium to allow microscopic observation of the bacteria. Mat samples were collected, and a minicore (1 cm in diameter and 1.5 cm deep) was taken from each mat sample. The resulting hole was filled with either 210- to 300-μm-diameter sterile glass beads or 250-μm-diameter sieved, sterile, nutrient-free 1.5% solid agar.

After 72 h, all surface water was pipetted off, and the mats were left for at least 2 h so that the sediment would dry slightly. Two glass coverslips were inserted vertically, about 1 mm apart, into the minicore and held in a wedge shape (as judged by eye). A cross-sectional, vertical, angular slice of the mat sediment and glass bead minicore was drawn up between the coverslips, and bacterial motility was analyzed in the minicore wedges. The coverslip slices were sealed horizontally onto a glass microscope slide, with petroleum jelly for stability and to prevent the entry of air and the loss of the mat sediment.

The cells were observed with an Olympus BH-2 compound microscope fitted with a video camera at a magnification of ×200. The motility of the cells was recorded with a video recorder, and the cell paths were analyzed frame by frame. A cell path was defined as the number of frames in which a motile cell remained in the focal plane (focal time). The speed, in micrometers per second, was then calculated for all cell paths to obtain an average speed for the sample. This technique was particularly useful in determining the speeds of very fast bacteria or bacteria whose path lengths were very short, as is the case in many bacterial swarms.

The bacterial community's motility and distribution were analyzed at depths of 10, 250, 500, 750, 1,000, and 1,500 μm in the minicore. The depth into the mat was calculated with the same conversion factor used to determine the lengths of the bacterial tracks.

Oxygen microelectrode measurements. The oxygen concentration was measured as a percentage of dissolved gas. This gives the value of 100% saturation for aerated seawater, equivalent to 260 μmol of dissolved oxygen liter^{-1}. The microelectrode (Diamond General Development Corp., Ann Arbor, Mich.) had a tip diameter of 50 μm. By using a technique adapted from that of Fenchel (8), the microelectrode was inserted with a micromanipulator and guided into the minicore by the use of the objective microscope. The microelectrode was inserted into the open end of the minicore wedge and sealed in position with petroleum jelly to prevent the entry of air, which might cause fluctuations in the oxygen concentration.

The signal from the microelectrode was amplified with a chemical microsensor (Diamond General). The electrode and microsensor were calibrated by using nitrogen-sparged sterile mat water as the zeroing sample and aerated sterile mat water as the sample with 100% atmospheric saturation. Five readings were taken for each depth, and these values were later averaged to give the percent oxygen saturation for each depth. After the mats had been exposed to darkness for 2 h, the percent oxygen saturation was measured again.

Community chemotaxis. To investigate bacterial behavior in oxygen and sulfide gradients, oxygenated sterile seawater and neutralized sodium sulfide (Na_2S) were added to the coverslip slices below the aerobic-layer microlamination in six independent experiments. The Na_2S was prepared at concentrations of 100, 200, 300, and 400 μmol liter^{-1} (18). The variations in oxygen concentration were achieved by autoclaving two 500-ml bottles of microbial-mat water (salinity, ~40 ‰). One of the bottles was bubbled with nitrogen for 30 min to expel all dissolved oxygen, while the second was bubbled with air. By using the microscope in conjunction with a micromanipulator, it was possible to guide the microcapillary tube between the coverslips by a method similar to the insertion of the microelectrode. The motility and concentration of bacteria near each microcapillary tube were then recorded to determine if the bacteria were responding to the new chemical concentration.

RESULTS

Figure 1a shows that over 45% of the total bacteria were swarming around a common depth of about 500 μm. These bacterial swarms, which extended uniformly throughout the horizontal plane of the mat, will be referred to as microlaminations to signify that they are not visible to the naked eye and to distinguish them from the classical plate and microcapillary swarms. Measurement of Fig. 1b shows a significant increase in bacterial abundance above the background, indicating that the microlamination began with a separation of 45 μm with a 13-μm-wide two-point peak.

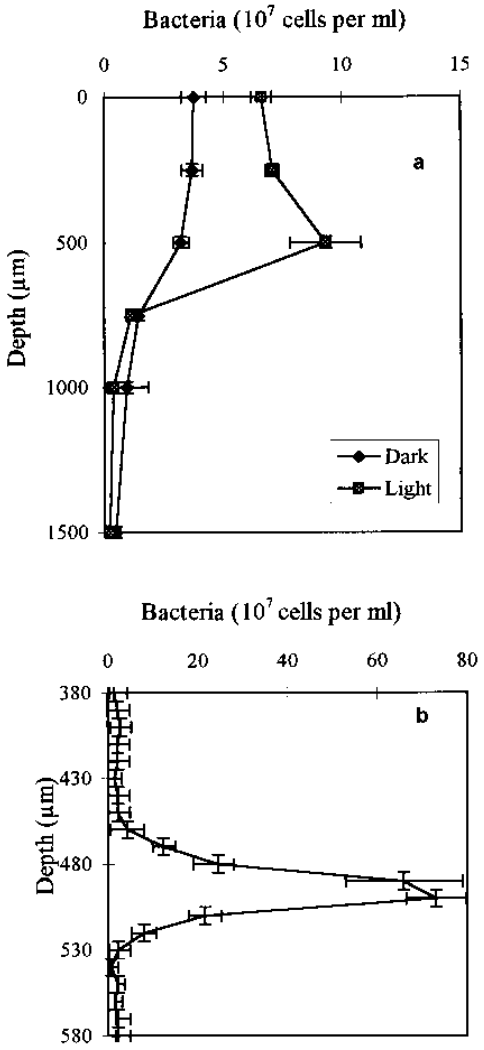

FIG. 1. (a) The average concentration of motile bacteria at each depth. Light and dark samples were measured 8 to 10 h apart within the same 24-h period. The horizontal error bars are 95% confidence intervals. The vertical error bars represent the depth range (20 μm) over which cell counts were performed for each point. Where error bars are not visible, they are smaller than the symbol. (b) The concentrations of motile bacteria measured at 10-μm intervals. The apparently high concentrations calculated for the center of the microlamination are due to the tight clustering of the bacteria in a small volume. The horizontal error bars are 95% confidence intervals. The vertical error bars represent the segment thickness (5 μm) over which cell counts were performed for this figure.

The low-resolution (250-μm) profile of the bacterial distribution (Fig. 1a) showed that the concentration of motile bacteria (average ± 95% confidence interval, $7.1 \times 10^7 \pm 3.0 \times 10^6$ cells ml^{-1} at 250 μm) increased to $9.3 \times 10^7 \pm 1.5 \times 10^7$ cells ml^{-1} at 500 μm. At 750 μm, the concentration decreased ninefold (to $1.1 \times 10^7 \pm 1.1 \times 10^6$ cells ml^{-1}). Higher-resolution counts (every 10 μm) of the bacterial distribution

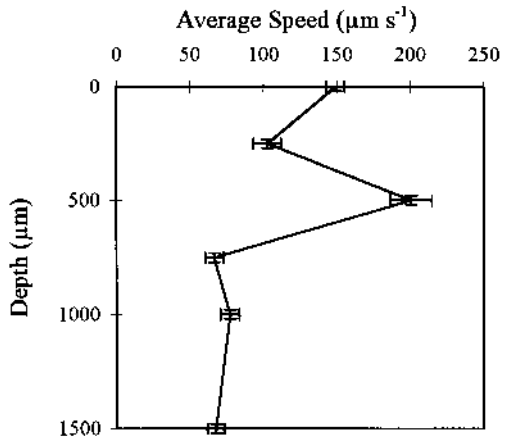

FIG. 2. Depth profile of the average bacterial speed in the minicore. The vertical error bars represent the segment thickness (20 μm) over which cell counts were performed for each point. The horizontal error bars are 95% confidence intervals.

around the microlamination revealed that the change in bacterial concentration was not gradual but instead occurred in a narrowly defined region around the 500-μm depth, with a threefold increase within only 10 μm (Fig. 1b).

The average community speed (200 ± 14 μm s^{-1}) peaked at a depth of 500 μm and then declined rapidly with increasing depth into the minicore (Fig. 2). The low-resolution profile of the turning frequency (Fig. 3a) shows that over 50% of the bacteria at 500 μm turned at least once per focal time. Investigation of the turning frequency at a higher resolution (every 10 μm) shows that percent turning peaked at 93% in the microlamination and dropped to 10% outside of the microlamination (Fig. 3b).

The mean focal time profile (Fig. 4) showed a trend opposite those of the average speed and turning frequency profiles, with reduced focal time at 500 μm. There was a significant decrease in mean focal time from 0.68 ± 0.06 s at 250 μm to 0.35 ± 0.05 s at 500 μm. The mean focal times for the bacterial community at 500 and 750 μm were tested with a two-tailed paired *t* test and found to be significantly different ($P = 0.002$). However, the focal times at depths of 500, 1,000, and 1,500 μm were not significantly different from each other.

Oxygen concentration. The oxygen profile (Fig. 5) of the minicore during daylight hours shows that the upper 250 μm was supersaturated with oxygen (157% ± 2.8% O_2 saturation). Percent O_2 saturation then declined steeply to zero at 550 μm. The average community speed measured peaked at 186 ± 15 μm s^{-1} at 500 μm, or 14% ± 0.8% O_2 saturation (Fig. 5). At 450 μm, 50 μm above the microlamination, the oxygen concentration was 32% ± 1.7% O_2 saturation, while 50 μm below the microlamination the oxygen concentration was only 3.8% ± 1.0% O_2 saturation. After 2 h of darkness, the anaerobic layer extended up to at least the 500-μm depth, where no sign of the microlamination was observed (data not shown).

Community chemotaxis. The addition of sulfide at a concentration of 100 or 400 μmol $liter^{-1}$ did not significantly affect the average community speed of bacteria within the minicore, nor did addition of oxygen-saturated seawater or deoxygenated seawater. However, at 300 μmol of sulfide $liter^{-1}$, the average community speed was significantly affected, increasing after 5 min from 52 ± 6.9 μm s^{-1} to 91 ± 20 μm s^{-1} (Fig. 6a). The initial increase in average speed in sulfide at 200 μmol $liter^{-1}$ was not as dramatic as that observed with sulfide at 300 μmol

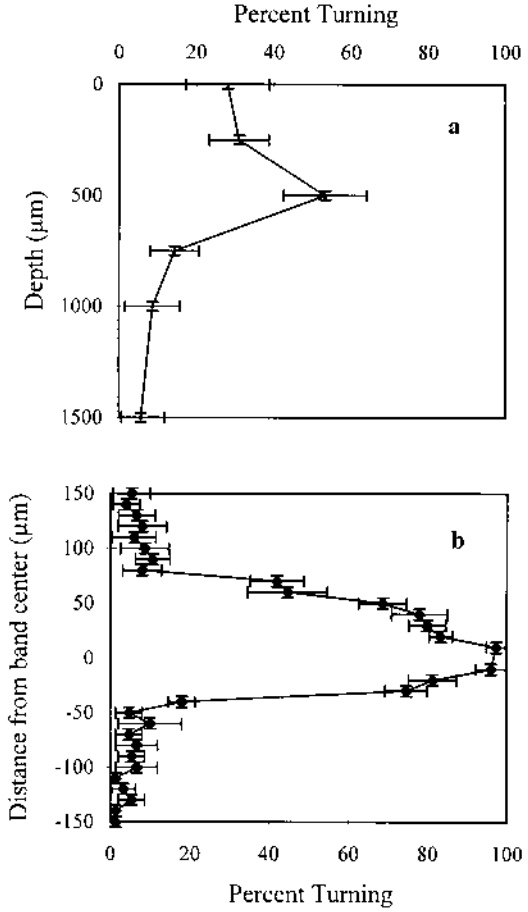

FIG. 3. (a) The percentage of turning bacteria, as measured for 300 bacteria at each depth. The vertical error bars represent the segment thickness (20 μm) over which cell counts were performed for each point. (b) The percentage of turning bacteria, measured at 10-μm intervals around the microlamination. The vertical error bars represent the segment thickness (5 μm) over which the counts were performed for this figure. The horizontal error bars in both panel a and panel b are 95% confidence intervals.

$liter^{-1}$. Instead, it appears to gradually rise over a 20-min period before declining back to 57 ± 7.2 μm s^{-1} (Fig. 6b). Figure 6d shows that the maximum concentration of motile bacteria was significantly influenced only by the addition of 200 μmol of sulfide $liter^{-1}$, in which case it increased from $1.5 \times 10^7 \pm 1.0 \times 10^6$ cells ml^{-1} to $7.1 \times 10^7 \pm 3.2 \times 10^6$ cells ml^{-1} (Fig. 6c).

DISCUSSION

The distribution of motile bacteria within the minicore was not uniform (Fig. 1a). Instead, bacteria were concentrated in a microlamination 500 μm below the mat surface. In the vicinity of the microlamination there was a marked change in bacterial behavior. The average community speed around the microlamination was almost 50 μm s^{-1} faster than at any other depth within the minicore. The turning frequency also increased significantly (Fig. 3a). This suggests that an increase in turning frequency around the microlamination may be a mechanism used to retain its integrity. This is in direct contrast to models of enteric chemotaxis, in which decreasing the turning frequency is the mechanism used for that function.

Significance of measuring resolution. The discovery of the microlamination within the minicore was made possible by the

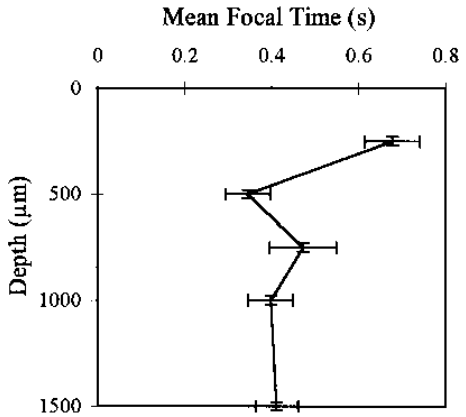

FIG. 4. The average time the bacteria were in focus (focal time) at different depths within the minicore. The focal time is defined as the number of seconds that a bacterium remained in the field of view, or focus. Short focal times correspond to a cell moving nearly perpendicular to the plane of focus. Because the slice through the minicores was perpendicular to the mat surface, short focal times mean that in the environment, bacteria were swimming parallel to the mat surface. The vertical error bars represent the segment thickness (20 μm) over which cell counts were performed for each point. The horizontal error bars are 95% confidence intervals.

high-resolution depth measurements. In previous studies, the maximum resolutions of depth measurements within mats were of the order of 100-μm increments (7, 9, 12, 17). This resolution is similar to that used in the low-resolution (250-μm) investigation of the minicores. However, previous studies were unable to detect microlaminations because sampling relied on dissection of mats to determine microbial abundances. The narrow (30- to 40-μm) width of the microlamination means that its dimensions are unlikely to be determined with a sampling resolution of 100 μm. This conclusion is supported by the differences in the sharpness of the microlamination when it is measured by the high- and low-resolution methods (Fig. 1a and b). If the mat was sampled only at 500 and 750 μm (Fig. 1a), it might appear that the bacteria steadily decrease in concentration. When the microlamination is examined in 10-μm increments, the resolution is increased, indicating that the bacterial-distribution gradient changes by a factor of 3 only 10 μm from the center of the band. If the sampling resolution was 1 μm, would there be an increase in the sharpness of the gradient?

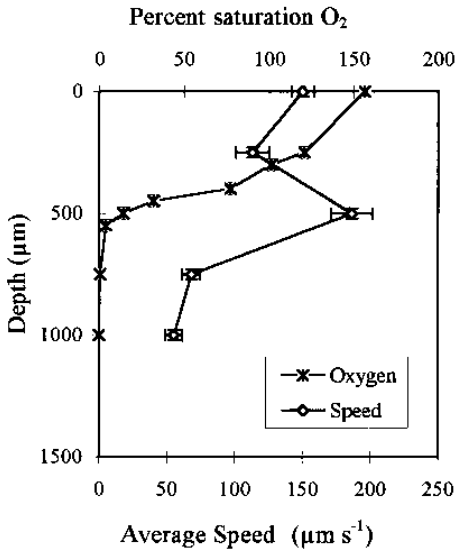

FIG. 5. Oxygen profile within a minicore plotted with average bacterial speed, measured during daylight. The oxygen concentration was measured as a percentage of dissolved gas, where aerated seawater is 100% saturation, equivalent to 21% dissolved O_2. The vertical error bars represent the segment thickness (20 μm) over which the measurements were performed for each point. The horizontal error bars are 95% confidence intervals.

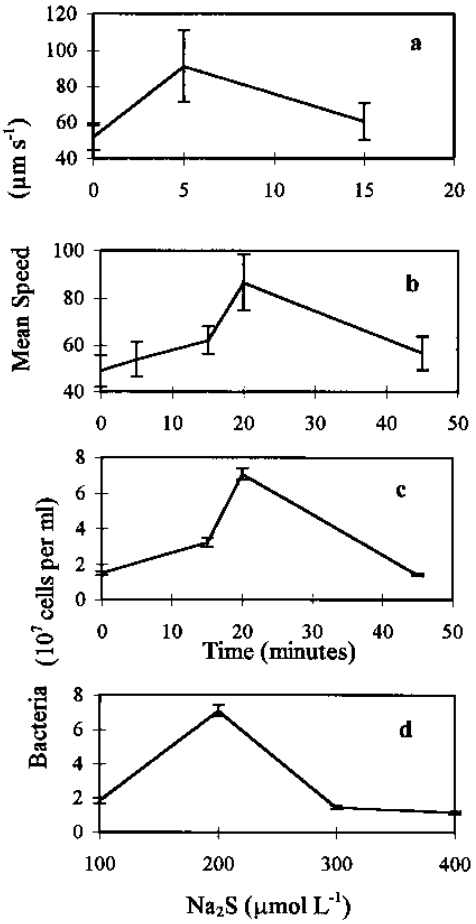

FIG. 6. The average bacterial speed in 300 μmol (a) and 200 μmol (b) of neutralized Na_2S $liter^{-1}$, plotted against time. (c) The average concentration of motile bacteria after the addition of 200 μmol of sulfide $liter^{-1}$. (d) The maximum concentration of motile bacteria as a function of the Na_2S concentration. The error bars are 95% confidence intervals.

Because bacteria are too short to sense a gradient over their body length, they must swim a minimum distance to detect a change in the chemical gradient (4). The minimum distance is determined by the equation $d = D/V$, where D is molecular diffusion ($\sim 10^{-5}$ cm s^{-2}) (3) and V is the average swimming velocity of the bacteria in the microlamination (2×10^{-2} cm s^{-1}); therefore, d = 5 μm.

At least two measurements are needed for a comparison of the chemical gradient, which means that at 200 μm s^{-1} the minimum distance would be 10 μm. This assumes, however, that at the start of every run each bacterium is positioned on the edge of the concentration within which it wants to remain (4). Deviations from this assumption, plus bacterial reaction time and the dynamic nature of the gradients within the mats, will expand the minimum distance to greater than 10 μm. For this reason it is unlikely that the microlamination could be

more than a factor of 2 narrower than the observed 30 to 40 μm.

The uniformity throughout the horizontal plane of the mat suggests that the bacteria position themselves within a microenvironment. What is the microenvironment in which the bacteria are swarming around, and what are the environmental cues that initiate the formation of the microlamination?

Ruling out light as a cue. Garcia-Pichel et al. (12) reported that light was the most important cue in triggering and modulating the migration of phototropic bacteria; however, they could not explain the migration patterns solely in terms of a light response. The possibility that light intensity is the major cue for the microlamination is unlikely for two reasons. First, if the bacteria were responding to light intensity, the structure of the microlamination would not be as narrow as it is. The minicores are translucent, and light is able to penetrate to the bottom layers; thus, a significant difference in light intensity just 500 μm below the surface is unlikely. Second, the fact that the bacteria did not alter swimming behavior after exposure to horizontal light for up to 1 h in the coverslip slices further supports the argument that bacteria were not responding to light.

Chemical gradients as cues. The bacterium *T. majus* is a large (5- to 25-μm) sulfur- and sulfide-oxidizing bacterium reported to have a chemosensory response to oxygen tension, resulting in the formation of a distinct swarm band of cells at a preferred oxygen concentration (8). The highly motile cells (600 μm s^{-1}) maintained the band by increasing their turning frequency around the preferred oxygen concentration within a sealed microslide (8). This type of behavior is similar to the increased speeds and turning frequency observed around the microlamination in this study. This suggests that the bacteria within the microlamination may have been orienting themselves in response to one of the chemical gradients (oxygen or sulfide) within the mat rather than to a change in light intensity.

Oxygen profile. The shape of the oxygen gradient within the minicore was consistent with the oxygen gradients obtained for other microbial mats. However, the anaerobic zone in the daylight extends up to 550 μm, which is much shallower than that of other mats (4 to 5 mm) (9, 17). This indicates that either the St. Kilda microbial mats have a high rate of oxygen respiration or the diffusion of oxygen into the minicore is slower than in microbial mats. It is unlikely that the minicores reduced the rate of oxygen diffusion, because their grain size was similar to that of the original sediment, so oxygen should diffuse as readily in the minicore as in the mat.

At St. Kilda, the mats have a high input of organic material from the mangrove forest; therefore, the productivity (rate of O_2 respiration) of the mat would also be high. The high rates of oxygen consumption would raise the aerobic-anaerobic boundary, enabling anoxygenic photosynthetic bacteria to receive more light and thus produce more sulfide. The increased sulfide concentration within the mat would become unstable, and the sulfide would in turn react with available oxygen to further decrease the oxygen concentration. The mats also contain organic matter in the form of live and lysing cells, as well as polysaccharides (9) which further slow the rate of diffusion. In the laboratory there was no input of organic matter into the mats, but the translucent properties of the minicores led to an increase in the penetration of light. Therefore, the raised aerobic-anaerobic boundary observed in the daylight measurements may be a result of an increased rate of sulfide production during anoxygenic photosynthesis.

The daylight oxygen measurements (Fig. 5) from the minicores showed that the microlamination was positioned within a steep oxygen gradient at 14% O_2 saturation (500 μm), below the O_2-supersaturated layer (150% O_2 saturation). After 2 h without light, the minicore oxygen concentration was almost half the maximum daylight concentration (data not shown), indicating that the oxygen concentration within the minicore was not static. Although the motility of the bacteria was not recorded during the O_2 measurements taken in the dark, it was noted that the microlamination was no longer present at 500 μm or at any of the other depths at which the oxygen concentration was recorded. The resolution of the O_2 measurements in darkness was not high enough to determine if the microlamination had migrated to another depth within the minicore. If the position of the microlamination was dependent on a narrow oxygen gradient, this would explain why the microlamination was no longer observed at the 500-μm depth. The bacteria within the microlamination may be able to survive only within a narrow range of O_2 tensions. Therefore, the change in the O_2 gradient from daylight to darkness would result in a shift in the position of microlamination as the bacteria followed the optimal oxygen tension.

Community chemotaxis. Bacteria responded to the addition of sulfide at 200 or 300 μmol $liter^{-1}$ by increasing their velocity but did not respond to sulfide at 100 or 400 μmol $liter^{-1}$, indicating that these bacteria can distinguish the sulfide concentration within a narrow range, of the order of 100 μmol $liter^{-1}$. The response of the bacteria to sulfide at 300 μmol $liter^{-1}$ was short-lived compared with that at 200 μmol $liter^{-1}$ (Fig. 6a and b). There are two possible explanations for this: (i) the bacteria were consuming the sulfide at an enhanced rate because of their increased speed and then slowing down as the concentration decreased; or (ii) the sulfide concentration may have become too high as the Na_2S solution diffused from the microcapillary tube, resulting in the migration of the bacteria to another gradient depth within the mat. The first explanation is unlikely, because the bacteria in sulfide at a concentration of 400 μmol $liter^{-1}$ would have had sufficient sulfide to enhance their average speed but did not do so. Support for the second explanation is provided by Fig. 6c and d. The bacteria did not increase in numbers with sulfide at 300 μmol $liter^{-1}$ despite their initial rapid increase in average speed (Fig. 6a), while at 200 μmol $liter^{-1}$ there was a sevenfold increase in the bacterial concentration. The bacterial response time to sulfide at 300 μmol $liter^{-1}$ was four times faster than that to sulfide at 200 μmol $liter^{-1}$ (Fig. 6a and b). After the average speed of bacteria in the presence of sulfide at 200 μmol $liter^{-1}$ had increased, the bacterial concentration where sulfide was at 200 μmol $liter^{-1}$ decreased back to concentrations comparable to those at time zero, suggesting that a threshold concentration must be reached before the speed of the bacteria increases. Therefore, the initial increase in average speed with the addition of sulfide at 300 μmol $liter^{-1}$ may be an avoidance response, with the increased speed serving as a vector to move the bacteria away from the increased sulfide as quickly as possible. To further test this theory, it would be necessary to use a sulfide microelectrode to take measurements near the tip of the microcapillary tube to determine if the concentration was increasing as more sulfide diffused from the tip or declining as it was being consumed by the bacteria.

In microbial mats, the change from anoxic to supersaturated oxygen conditions occurs over vertical distances of a few millimeters, or at most a centimeter, and fluctuates on a diurnal cycle. Therefore, microorganisms within these environments need to be able to respond to the changes in the chemical gradients not only on a spatial scale but also on a temporal scale. The rate at which bacteria respond to the fluctuations is of foremost importance in their ability to survive within the

mats and ultimately determines the structure and composition of the mat. The microlamination represents a narrow region (30 to 40 μm) in the mat where it appears that heterotrophic bacteria depend on the simultaneous presence of sulfide and oxygen gradients as chemical signals to maintain the integrity of this thin structure.

The narrowness of the microlamination indicates that bacteria within the mat are capable of responding to small changes in chemical gradients by increasing their turning frequency (Fig. 6a to c and 3b). In the past, the resolution of measurements made on mats was too low to detect the presence of the microlaminations (7, 9). They may have also failed to detect actual chemical-gradient changes in the mats. In future studies, higher-resolution sampling when measuring chemical gradients and bacterial distributions within mats is warranted. This would increase the likelihood that microstructures within mats are accurately quantified, providing a representative picture of the mat ecosystem.

The in situ measurements of motility performed in this study allowed the quantification of bacterial motility not only for a single species but for the entire heterotrophic community within the minicore. However, the applications of this technique are not limited to microbial mats. The community motility methods used in this study could be applied to other bacterial communities that experience high levels of bacterial competition for nutrient sources. For example, in subterranean aquifers (14), the motility of bacteria within mixed communities may increase their competitive fitness (13).

REFERENCES

1. **Adler, J.** 1966. Chemotaxis in bacteria. Science **153:**708–716.
2. **Bauld, J.** 1981. Geobiological role of cyanobacterial mats in sedimentary environments: production and preservation of organic matter. BMR J. Aust. Geol. Geophys. **6:**307–317.
3. **Bauld, J.** 1984. Microbial mats in marginal marine environments Shark Bay, Western Australia, and Spencer Gulf, South Australia, p. 39–58. *In* R. W. Castenholtz, Y. Cohen, and H. O. Halverson (ed.), Microbial mats: stromatolites. Alan R. Liss, Inc., Canberra, Australia.
4. **Berg, H. C.** 1983. Random walks in biology. Princeton University Press, Princeton, N.J.
5. **Cohen, Y.** 1989. Photosynthesis in cyanobacterial mats and its relationship to the sulfur cycle: a model for microbial sulfur interactions, p. 22–36. *In* Y. Cohen and E. Rosenberg (ed.), Microbial mats: physiological ecology of benthic microbial communities. American Society for Microbiology, Washington, D.C.
6. **Cohen, Y., and E. Rosenberg (ed.).** 1989. Microbial mats: physiological ecology of benthic microbial communities. American Society for Microbiology, Washington, D.C.
7. **D'Antoni D'Amelio, E., Y. Cohen, and D. J. Des Marais.** 1989. Comparative functional ultrastructure of two hypersaline submerged cyanobacterial mats: Guerrero Negro, Baja California Sur, Mexico, and Solar Lake, Sinai, Egypt, p. 97–113. *In* Y. Cohen and E. Rosenberg (ed.), Microbial mats: physiological ecology of benthic microbial communities. American Society for Microbiology, Washington, D.C.
8. **Fenchel, T.** 1994. Motility and chemosensory behaviour of the sulphur bacterium *Thiovulum majus*. Microbiology **140:**3109–3116.
9. **Fenchel, T., and B. J. Finlay.** 1995. Ecology and evolution in anoxic worlds. Oxford University Press, Oxford.
10. **Fründ, C., and Y. Cohen.** 1992. Diurnal cycles of sulfate reduction under oxic conditions in cyanobacterial mats. Appl. Environ. Microbiol. **58:**70–77.
11. **Garcia-Pichel, F.** 1989. Rapid bacterial swimming measured in swarming cells of *Thiovulum majus*. J. Bacteriol. **171:**3560–3563.
12. **Garcia-Pichel, F., M. Mechling, and R. W. Castenholz.** 1994. Diel migrations of microorganisms within a benthic, hypersaline mat community. Appl. Environ. Microbiol. **60:**1500–1511.
13. **Kelly, F. X., K. J. Dapsis, and D. A. Lauffenburger.** 1988. Effect of bacterial chemotaxis on dynamics of microbial competition. Microb. Ecol. **16:**115–131.
14. **McCaulou, D. R., R. C. Bales, and R. G. Arnold.** 1995. Effect of temperature-controlled motility on transport of bacteria and microspheres through saturated sediment. Water Resour. Res. **31:**271–280.
15. **Mitchell, J. G., M. Martinez-Alonso, J. Lalucat, I. Esteve, and S. Brown.** 1991. Velocity changes, long runs and reversals in the *Chromatium minus* swimming response. J. Bacteriol. **173:**997–1003.
16. **Phillips, B. R., J. A. Quinn, and H. Goldfine.** 1994. Random motility of swimming bacteria: single cells compared to cell populations. Am. Inst. Chem. Eng. J. **40:**334–348.
17. **Revsbech, N. P., P. B. Christensen, and L. P. Nielsen.** 1989. Microelectrode analysis of photosynthetic and respiratory processes in microbial mats, p. 153–162. *In* Y. Cohen and E. Rosenberg (ed.), Microbial mats: physiological ecology of benthic microbial communities. American Society for Microbiology, Washington, D.C.
18. **van Germeden, H., and H. H. Beeftink.** 1983. Ecology of phototrophic bacteria, p. 146–185. *In* J. G. Omerod (ed.), The phototrophic bacteria: anaerobic life in the light. Blackwell Scientific Publications, Oxford.